

Original Research

## Sustainable Synthesis of Zeolitic Imidazolate Framework-8 Nanoparticles and Application in the Adsorption of the Drug Chlorhexidine

Heloísa Maria de Oliveira <sup>†</sup>, Francisco Alex de Sousa Silva <sup>†</sup>, Tellys Lins Almeida Barbosa <sup>†</sup>, Meiry Gláucia Freire Rodrigues <sup>†,\*</sup>

Universidade Federal de Campina Grande, Unidade Acadêmica de Engenharia Química, 58109-970 Campina Grande-PB, Brazil; E-Mails: [heloisa.oliveira@eq.ufcg.edu.br](mailto:heloisa.oliveira@eq.ufcg.edu.br); [francisco.sousa@eq.ufcg.edu.br](mailto:francisco.sousa@eq.ufcg.edu.br); [tellyslins@hotmail.com](mailto:tellyslins@hotmail.com); [meiry.freire@eq.ufcg.edu.br](mailto:meiry.freire@eq.ufcg.edu.br)

<sup>†</sup> These authors contributed equally to this work.

\* **Correspondence:** Meiry Gláucia Freire Rodrigues; E-Mail: [meiry.freire@eq.ufcg.edu.br](mailto:meiry.freire@eq.ufcg.edu.br)

**Academic Editor:** Narendra Kumar

**Special Issue:** [Applied Catalysis for a Circular Economy](#)

*Catalysis Research*

2023, volume 3, issue 1

doi:10.21926/cr.2301012

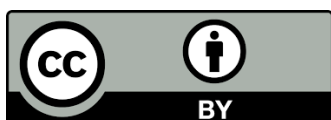
**Received:** December 06, 2022

**Accepted:** March 08, 2023

**Published:** March 13, 2023

### Abstract

In an attempt to synthesize nanomaterial concerning chemistry, the sustainable synthesis of Zeolitic Imidazolate Framework-8 (ZIF-8) nanoparticles by a low-cost approach through the recycling of waste mother liquors was explored and then indicated the potential to remove chlorhexidine (CHLX) from an aqueous solution. ZIF-8 was produced under solvothermal reaction at 25°C and characterized by Fourier Transform Infrared Spectroscopy, X-ray diffraction, adsorption/desorption of N<sub>2</sub>, dynamic light scattering and contact angle. The water Chemical stability test was conducted using ZIF-8 and it was immersed in pure water for 24 h at room temperature. Batch-type adsorption was used to check the potential of ZIF-8 (first and second generation) for the adsorption of the chlorhexidine with initial chlorhexidine concentration (0.05, 0.06 and 0.07 mol/L), agitation time (1, 3.5 and 6 h) and the mass of nano-adsorbent (0.04, 0.05 and 0.06 g). Process optimization was performed through a Factorial experimental design. The optimum conditions were selected for the nano-



© 2023 by the author. This is an open access article distributed under the conditions of the [Creative Commons by Attribution License](#), which permits unrestricted use, distribution, and reproduction in any medium or format, provided the original work is correctly cited.

adsorbent mass of 0.04 g, agitation time of 1 h and initial chlorhexidine concentration 0.07 mmol/L. The ZIF-8 sustainable synthesis was efficient and generated a crystalline nanomaterial. The result shows that ZIF-8 is stable in water under ambient conditions. The ZIF-8 first generation and ZIF-8 second generation exhibit a high adsorption capacity (27.17 mg/g and 30.96 mg/g). It was found that, under the synthesis conditions, the recycled mother liquor user did not affect the final characteristics of this nanomaterial. The results indicated that the initial concentration of chlorhexidine and nano-adsorbent mass influenced the adsorption capacity. Experimental design provided the process optimum conditions (1 h, 0.04 g of adsorbent mass and 0.07 mmol/L).

### Keywords

Zeolitic imidazolate frameworks (ZIF); recycled mother liquor; sustainable synthesis; chlorhexidine; adsorption

## 1. Introduction

Contamination caused by industrial pharmaceutical production has become a universal problem that affects the entire ecosystem [1].

Dangerous factors caused by environmental pollution from the pharmaceutical industry are emerging contaminants and many well-identified species such as pharmaceuticals and personal care products (PPCPs) [2-4].

Pharmaceuticals play a crucial aspect in health care. They are neither biodegradable nor chemically destroyed and are generally detected in surface water, groundwater and drinking water, and wastewater [5-7].

Several procedures for removing pharmaceuticals from wastewater have been developed, such as membrane filtration, adsorptive treatment, and chemical and photochemical oxidation processes. However, the high cost associated with and most of these methods has become a limiting factor in their utilization [5].

Alternatives for classical treatment technologies are crucial to become better the elimination of pharmaceuticals from aqueous solutions. Today, adsorption has become a promising choice for treating pharmaceuticals from wastewater. Adsorption is considered an efficient procedure to remove micro-pollutants, producing high-quality effluents. The major benefits associated with adsorption are cost-effectiveness, high efficiency, regeneration of the adsorbent, low consumption of reagents, and the possibility of pharmaceutical recovery [8-11].

Metal-Organic frameworks (MOFs) are highly ordered porous crystalline materials with high porosity and large specific surface area [12]. Zeolitic imidazolate frameworks (ZIFs) are one of the most relevant classes of these MOFs and one of the diverse types of ZIFs [13]. ZIFs are three-dimensional structures with tetrahedral topologies, built by divalent metal cations ( $Zn^{2+}$ ,  $Co^{2+}$ ,  $Cu^{2+}$ ) connected by imidazolate anions and/or their derivatives (imidazole, 2-methylimidazole, benzimidazole) [14].

ZIF-8 [ $Zn(C_4H_5N_2)_2$ ] is a tetrahedral structure formed by zinc ions and imidazolate ligands, has high chemical and thermal stability, considerable accessible surface area, and abundant active

surface sites [14, 15]. An advantage of ZIF-8 nanoparticles is their excellent stability, enabling long-term operation [16]. In recent years, several chemical routes for producing ZIFs have been developed. Among the main methods is synthesizing organic solvents called – solvothermal [17]. However, due to the energy crisis and organic solvents that lead to environmental risks, considerable studies and efforts have been dedicated to creating sustainable synthesis routes for ZIFs to minimize the environmental effects [18].

During the reaction mixture process of ZIF-8 in the solvothermal procedure, the nanocrystals, obtained by precipitation, are separated by centrifugation of the supernatant (mother liquor). The mother liquor is a mixture rich in organic and inorganic species and is usually discarded, promoting waste and possible contamination of water resources. Some authors argue that it is possible to reuse the mother liquor as a reagent in synthesizing porous materials, thus promoting resource sustainability and environmental protection [19-23].

ZIF-8 based on  $Zn^{2+}$  due to its low toxicity and good biocompatibility has attracted important attention in various applications, mainly gas storage, contaminant adsorption [24-27] and drug delivery [28, 29].

Authors [28] developed and characterized a BNZ@ZIF-8 system. The modulation of BNZ release from the ZIF-8 framework was evaluated through the in vitro dialysis release method under sink conditions at different pH values. Moreover, the in vitro evaluation of cell viability and cytotoxicity by MTT assay was also performed. The dissolution studies corroborated that a pH-sensitive Drug Delivery System capable of vectorizing the release of BNZ was developed, which may lead to the improvement in the bioavailability of BNZ. The MTT assay showed no statistically significant toxic effects in the developed system or significant effects on cell viability.

Results of the review reported by authors [29] demonstrated the preparation and functional modification of ZIF-8, and its application in drug delivery, focusing on the single-stimulus and multi-stimulus response release of drugs in ZIF-8 materials, the integrated role of diagnosis and treatment with ZIF-8 in cancer treatment, and its application in the synergistic therapy of multiple cancer treatment methods.

Certain drugs are included in the class of emerging contaminants because, when present in water resources, they are persistent to conventional treatments [30]. Chlorhexidine (CHLX) is a biguanide antiseptic and cationic compound widely used in various health sectors, in addition to drug production and it is widely used in dentistry for plaque prevention [31].

From the environmental point of view, the appropriate management of waste allows for the reduction of detrimental impacts on the environment. So, in this work, to reduce production costs and promote the recycling of the mother liquor (the mother liquor is expected to contain a substantial amount of unused  $Zn^{2+}$ , 2-methylimidazole and methanol), a methodology was developed for the synthesis of ZIF-8 using mother liquor and to evaluate the adsorption of chlorhexidine. In this work, we examined the influence of agitation time (t), nano-adsorbent mass (m) and initial solution concentration on CHLX ( $C_0$ ) onto ZIF-8 using a factorial experimental design.

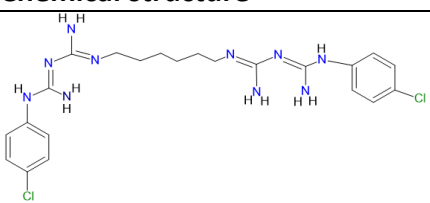
## 2. Materials and Methods

All chemicals and solvents were purchased from commercial suppliers and used as received, including zinc nitrate hexahydrate  $Zn(NO_3)_2 \cdot 6H_2O$ , Acros Organics, 98.0 %, 2-methylimidazole

(CH<sub>3</sub>C<sub>3</sub>H<sub>2</sub>N<sub>2</sub>H, Aldrich, 99.0%), methanol P. A. (CH<sub>3</sub>OH, Neon, 99.9%). Chlorhexidine (C<sub>22</sub>H<sub>30</sub>Cl<sub>2</sub>N<sub>10</sub>) was supplied by Merck.

The properties of chlorhexidine are given in Table 1.

**Table 1** Overview of physicochemical properties of the chlorhexidine.

	Molecular formule	Chemical structure	Molecular mass
Chlorhexidine	C <sub>22</sub> H <sub>30</sub> Cl <sub>2</sub> N <sub>10</sub>		505.4 g/mol

### 2.1 Preparation of ZIF-8 1G Crystals

ZIF-8 was prepared by a solvothermal procedure based on changes made to the conventional method described by the authors [17]. A solution of zinc nitrate hexahydrate (9.88 mmol) was dissolved in methanol (200 ml), named solution (A) and remained under stirring with a magnetic bar for 30 min. A solution of 2-methylimidazole (79.17 mmol) was dissolved in methanol (200 ml), named solution (B) and remained under stirring with a magnetic bar for 30 min. The clear solution (B) was poured into the former clear solution (A). The mixture quickly turned turbid and it was stirred magnetically at a room temperature of 25°C for 1 h. The nanocrystals were separated from the milky dispersion by centrifugation (3400 rpm for 15 min) using a Cole-Parmer fixed-speed centrifuge. ZIF-8 was washed with methanol (10 ml) and centrifugated (3400 rpm for 15 min) two times. The nanocrystals were dried in an oven (Quimis) at 60°C for 24 h. The sample was prepared with the following molar composition: Zn(NO<sub>3</sub>)<sub>2</sub>·6H<sub>2</sub>O:8CH<sub>3</sub>C<sub>3</sub>H<sub>2</sub>N<sub>2</sub>H:1000CH<sub>3</sub>OH. The as-prepared sample was denominated ZIF-8 1G.

### 2.2 Preparation of ZIF-8 Crystals from Recycled Mother Liquors

In this study to reduce production costs and promote the recycling of the mother liquor (the mother liquor is expected to contain substantial amount of unused Zn<sup>2+</sup>, 2-methylimidazole and methanol), a methodology was developed for the synthesis of ZIF-8 using mother liquor.

The synthesis of the nanomaterial in consecutive generation (ZIF-8 2G) occurred equivalently to the procedure previously described. However, the recycled mother liquor (ML) collected in the solvothermal preparation of ZIF-8 1G was added during the initial stage of the synthesis without alterations, replacing the mass corresponding to the methanol needed to form the reaction mixture. The as-prepared sample was named ZIF-8 2G.

Figure 1 is shown the flow diagram preparation of ZIF-8 (first generation (ZIF-8 1G) and second generation (ZIF-8 2G)).

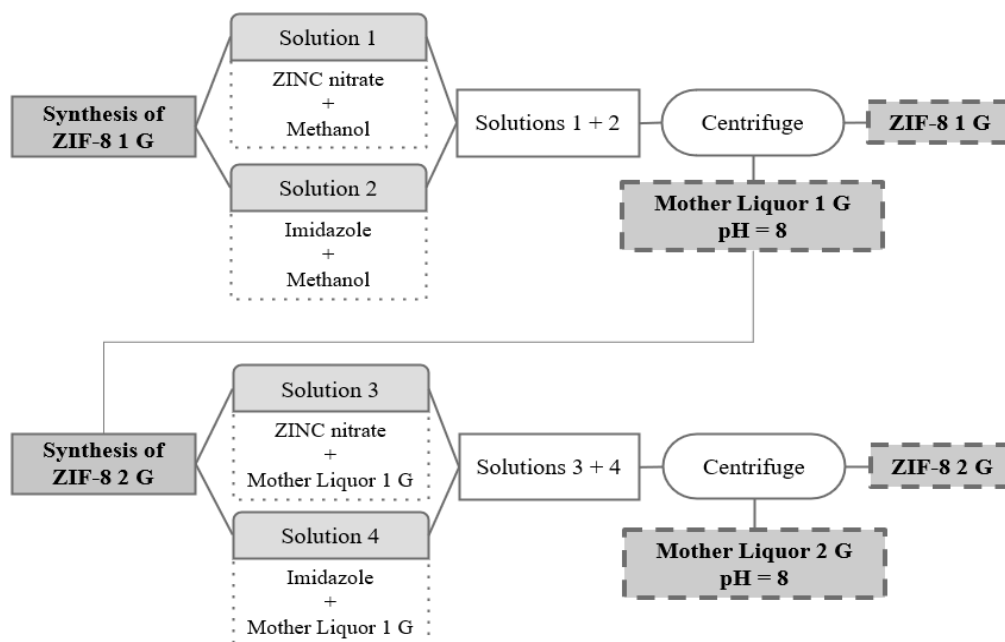


**Figure 1** Schematic diagram synthesis of ZIF-8 (first generation and second generation).

### 2.3 Characterization

X-ray diffraction patterns were carried out on a Shimadzu XRD 6000 using Cu K $\alpha$  radiation at 40 kV/30 mA, with a goniometer velocity of 2 $^{\circ}$ .min $^{-1}$  and step of 0.02 $^{\circ}$  in the 2 $\theta$  range from 3.0 $^{\circ}$  to 50.0 $^{\circ}$ .

FT-IR VERTEX 70 MODEL (Bruker) was used to obtain the infrared. The IR spectra were obtained at wavelengths in the 4000-400 cm $^{-1}$  range with a resolution of 4 cm $^{-1}$ .

The textural characteristics of the analyzed sample were investigated by isothermal gas adsorption/desorption of N $_2$  at 77 K using a Micro metrics ASAP 2020 equipment (Micromeritics).

The mean diameter analysis of ZIF-8 was performed using the light scattering technique of the hydrodynamic ray or dynamic light scattering (DLS), and zeta potential measurements were carried out on a HORIBA Scientific SZ-100.

The contact angle (CA) for ZIF-8 was taken on Phoenix-I portable contact angle from Surface Electro Optics- SEO was used to measure the angle of the water drop (H $_2$ O) when falling on the surface of the ZIF-8.

### 2.4 Chemical Stability

The procedure to determine the chemical stability of ZIF-8 was based on the methodology presented in the literature [14]. Stability tests of ZIF-8 1G were conducted by adding a given amount of ZIF-8 1G into distilled water at a predetermined ZIF-8 to water mass ratio in a beaker. The beaker was sealed and stirred for 24 h at room temperature (25  $\pm$  3 $^{\circ}$ C). Afterward, the suspended powder was collected by removing water by evaporation in a stove at 60 $^{\circ}$ C for 24 h. The obtained water-treated product was stored in a desiccator.

### 2.5 Reaction Yield (RY)

Yield was calculated from Equation 1

$$RY = \frac{m_{ZIF-8,Exp}}{m_{ZIF-8,Max}} \cdot 100 \quad (1)$$

Where:  $m_{ZIF-8, Exp}$  is the mass of solid product obtained experimentally (g);  $m_{ZIF-8, Max}$  is the mass of product that can be obtained if all the limiting reactant is consumed (g).

## 2.6 Adsorption

All adsorption tests were carried out using a shaker table (Certomat® MO, Biotech International, German) at 200 rpm under the temperature of 25°C. The adsorption of CHLX was studied under the following experimental conditions: CHLX with an initial concentration (0.05 mg/L, 0.06 mg/L and 0.07 mg/L, ZIF-8 powder (0.04 g, 0.05 g and 0.06 g); and agitation time of 1 h, 3.5 h and 6 h. Afterward, the solutions were centrifuged and then the residual CHLX in an aqueous solution was analyzed by UV-vis spectrophotometer (UV-VIS 1600 Pro-Analysis) at 260 nm.

## 2.7 Determination of the Amount of CHLX

The quantity of adsorbed CHLX per unit mass of ZIF-8, can be obtained by Equation (2)

$$q_{eq} = \left( \frac{C_0 - C}{m} \right) \cdot V \quad (2)$$

Where:  $q_{eq}$  is adsorption capacity (mg/g);  $V_{CHLX\ solution}$  (L) is the total volume of CHLX solution;  $m_{ZIF-8}$  (g) denotes the mass of ZIF-8;  $C_0$  (mmol/L) is the initial CHLX concentration, and  $C$  (mmol/L) is the final CHLX concentration after removal.

## 2.8 Factorial Experimental Design

A level factorial experimental design with three replicates in the central point was applied. Three independent variables were selected: the initial concentration of CHLX solutions ( $C_0$ ), evaluated in the range of 0.05 to 0.07 mmol/L, the agitation time ( $t$ ) kept within the range from 1 to 6 h and the nano-adsorbent mass kept with the range 0.04 to 0.06 g. According to the proposed factorial experimental design, the factor levels were coded as follows: i) 0.06 g, 0.07 mmol/L and 6 h associated with the high level, denoted “+1”; ii) 0.04 g, 0.05 mmol/L and 1 h, corresponding to the low level, denoted “-1”; and iii) the central points, 0.05 g, 0.06 mg/L and 3.5 h, denoted “0” [32].

MINITAB release 19.1 statistical software was employed to create and evaluate the experimental data, and to measure the effect of different parameters influencing the elimination of CHLX.

## 3. Results and Discussion

### 3.1 Characterization

Figure 2 shows the diffractograms of the ZIF-8 prepared initially (ZIF-8 1G) and from the following ZIF-8 2G and XRD simulated.

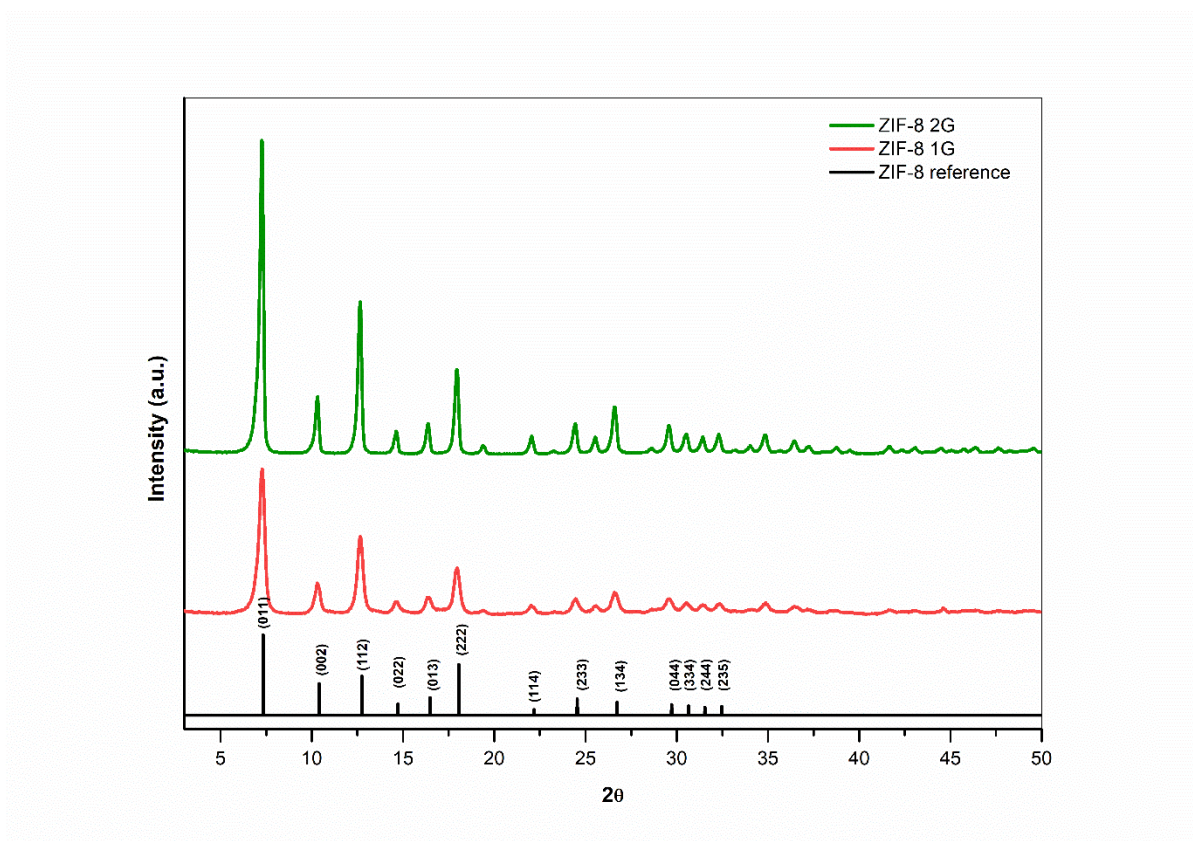


**Figure 2** XRD spectra of the as-synthesized ZIF-8 (first generation and second generation) and simulated.

The formation of two samples (ZIF-8 1G and ZIF-8 2G) was confirmed by the XRD analysis as shown in Figure 2 which indicates the formation of highly crystalline ZIF-8. Two samples (ZIF-8 1G and ZIF-8 2G) almost show the same XRD patterns and exhibit six evident peaks at  $7.53^\circ$ ,  $10.58^\circ$ ,  $12.93^\circ$ ,  $14.84^\circ$ ,  $16.67^\circ$  and  $18.24^\circ$ , corresponding to the (011), (002), (112), (022), (013), and (222) planes of ZIF-8, respectively (JCPDS 00-062-1030) [14, 17, 33, 34]. This indicates that the two samples have the same phase of ZIF-8 and the mother liquor does not change the structure of the prepared ZIF-8.

The spectra of the two generations (ZIF-8 1G and ZIF-8 2G) are presented in Figure 3.



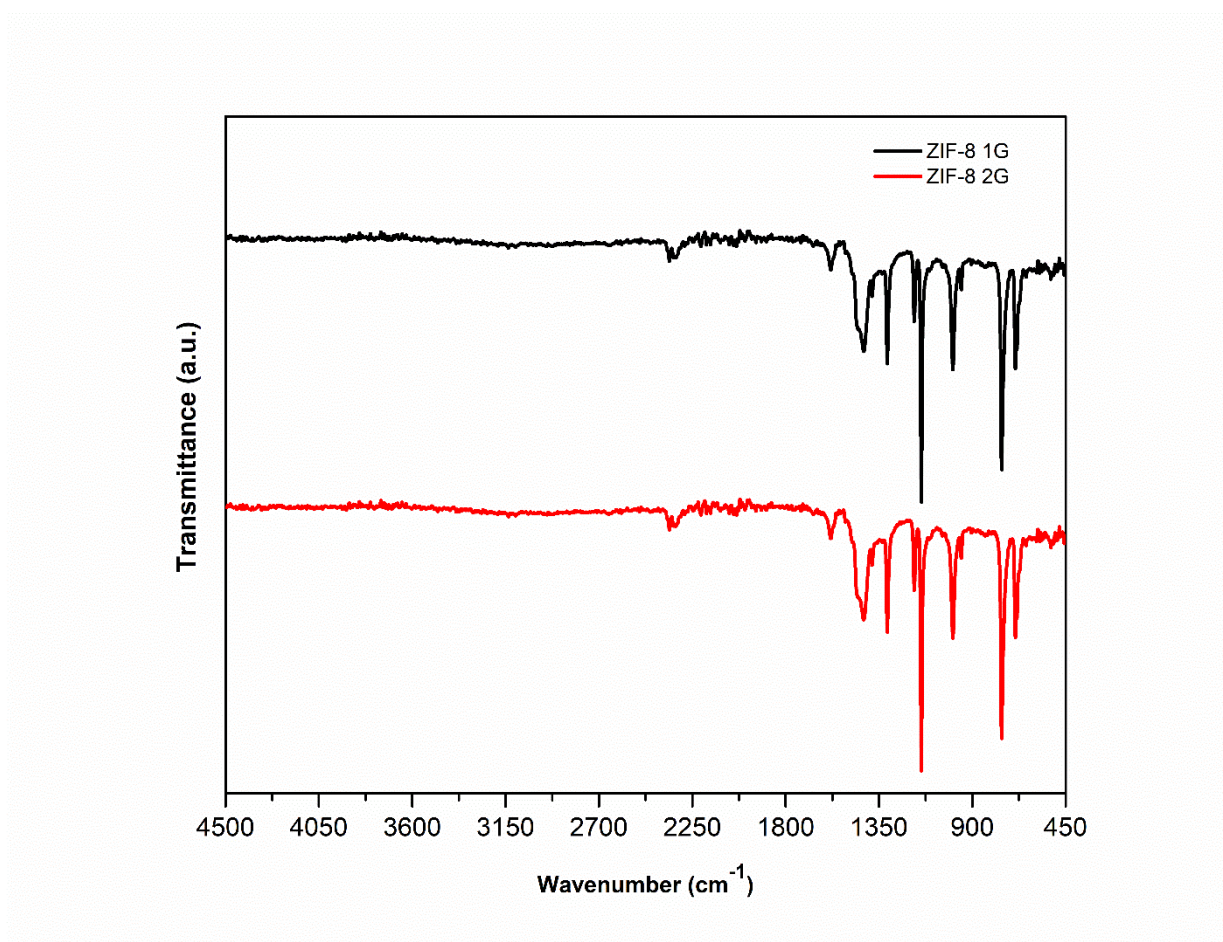


**Figure 3** FTIR spectra of the as-synthesized ZIF-8 (first generation and second generation).

For the (ZIF-8 1G and ZIF-8 2G) nanoparticles, there are characteristic bands at 3134 and 2927 cm<sup>-1</sup> were associated with the aromatic C–H and aliphatic C–H bonds, respectively, and the band around 1583 cm<sup>-1</sup> is related to stretching C=C. The bands in the region between 1100 and 1400 cm<sup>-1</sup> represent the adsorption bands C–H, C=N, and C–N in the imidazole ring, respectively. The band related to the stretching of the Zn–N bond is around 420 cm<sup>-1</sup> [5]. These results are consistent with the literature [5, 35].

Particle size distribution of ZIF-8 1G was obtained from DLS analysis (Figure 4). It can observe distribution curves with the monomodal profile.



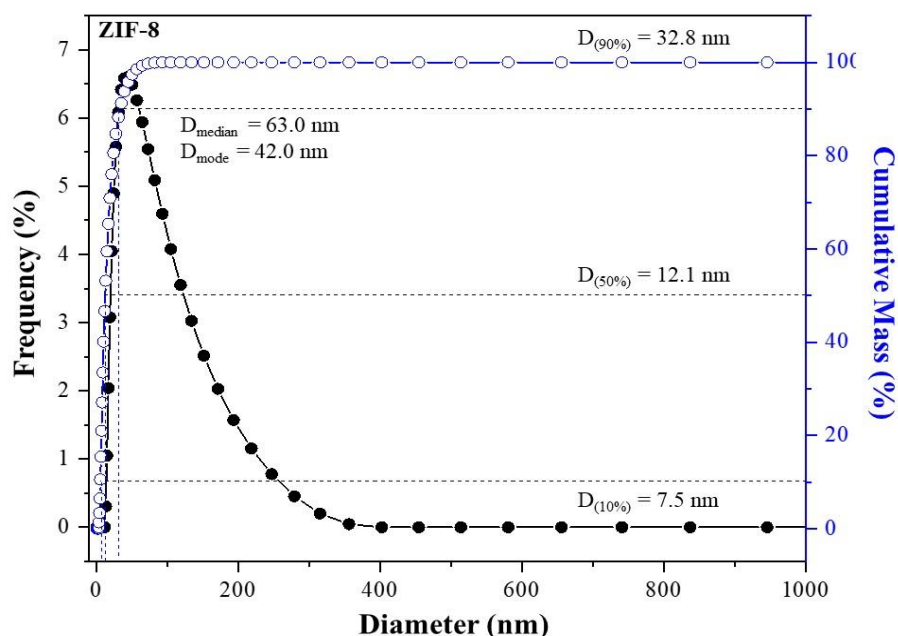


**Figure 4** Particle size distribution of ZIF-8 1G.

The diameter of the particles was found to be 63.0 nm. In this kind of distribution, the parameter  $D_{50\%}$  represents the particle of median value, that is, the particle dimension that separates the 50% of the finer particles from the 50% of the largest particles, whose average value was 12.1 nm. The values of  $D_{10\%}$  and  $D_{90\%}$  were 7.5 and 32.8 nm, respectively, representing a relatively narrow distribution range.

The surface charge (zeta potential), measured at pH 7.0 (neutral), was -48.0 mV. It was observed that ZIF-8 1G consists of negatively charged nanoparticles.

The contact angle value for the ZIF-8 1G is  $97^\circ$ . This value shows that the sample is hydrophobic with water, which must come mainly from its hydrophobic compositions of imidazolate rings. This result is in agreement with the literature [36].

### 3.2 Chemical Stability (Analysis of Product Collected by Drying)

The chemical stability of ZIF-8 1G was checked by suspending samples of ZIF-8 1G in water (Figure 5). ZIF-8 1G sample was immersed in the water for 24 h at room temperature.

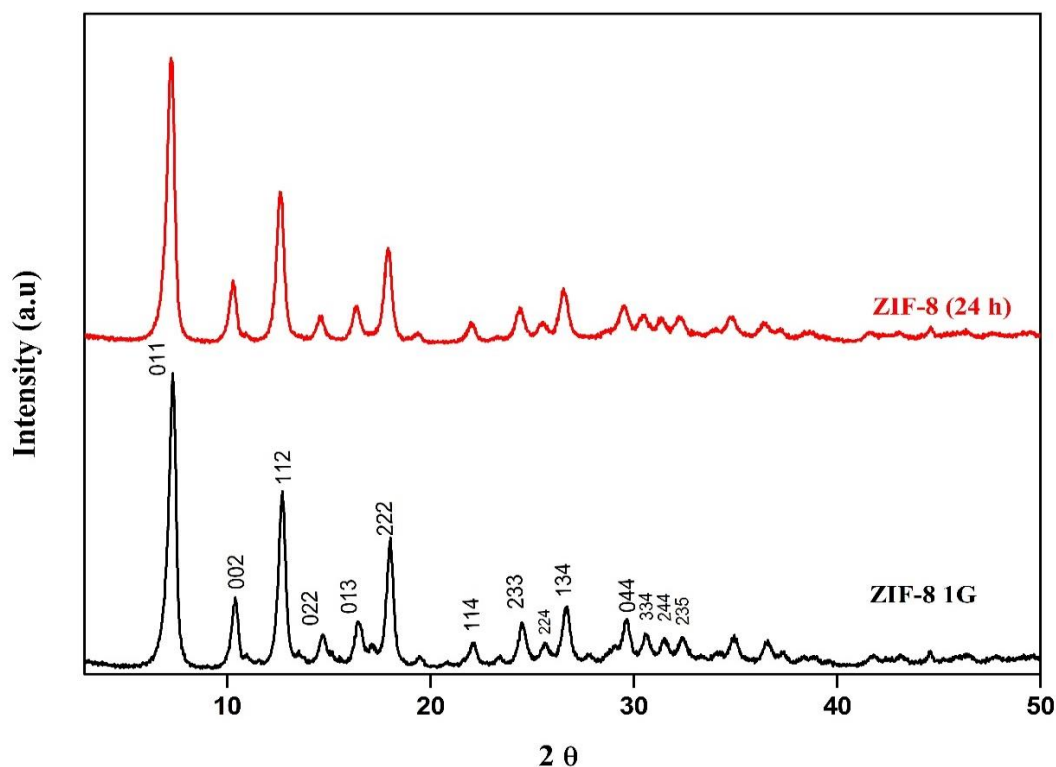


**Figure 5** XRD patterns of ZIF-8 and their corresponding product after water treatment.

ZIF-8 1G after the stability test, shows essentially the same crystalline structure from XRD data in Figure 5. ZIF-8 1G sustained their structure in water at room temperature for 24 h. Such observations are consistent with the literature [36-38]. The drying treatment for the stability-tested sample was done just 60°C. Such a lower temperature is less likely to lead to the phase transformation of ZIF-8.

### 3.3 Reaction Yield (RY)

The data obtained in this study on the reaction yield (RY) of the ZIF-8 1G and ZIF-8 2G are shown in Table 2 and other literature.

**Table 2** Main Parameters of ZIF-8 1G and Recycled Product (ZIF-8 2G).

Sample	RY (%)	BET surface area (m <sup>2</sup> /g)	Average particle diameter (nm)	Reference
ZIF-8 1G	47.08	1003	63.00	This work
ZIF-8 2G	11.75	-	-	This work
ZIF-8 1G	38.00	1773	31.00	[20]
ZIF-8 2G	37.00	515	27.00	[20]
ZIF-8	30.00	-	-	[39]

The yield value of the first-generation ZIF-8 1G was 47.08%. This value is higher than the yield values found by the authors [20, 39] who presented yields of 38.00% and 30.00%, respectively. However, the yield value of ZIF-8 obtained by the sustainable route (or 2nd generation) was 11.75%, a much lower value than the value found for the synthesis of ZIF-8 prepared in the first generation

(47.08%). This demonstrates that the yield of ZIF-8 is precisely touched by using the mother liquor. A solution to solve this problem would be to treat the mother liquor (the mother liquor is expected to contain a substantial amount of unused  $Zn^{2+}$ , 2-methylimidazole and methanol) with NaOH or  $NH_4OH$ , as demonstrated by the authors [20].

The specific area and average particle diameter values obtained for the ZIF-8 1G were  $1003 \text{ m}^2/\text{g}$  and  $63.00 \text{ nm}$ . The pH value of the mother liquor was 8.0. The value of the specific surface area in the present study is most likely unaffected, since the pH value was not modified.

In the literature, specific area and average particle diameter values found were  $1773 \text{ m}^2/\text{g}$  and  $31.00 \text{ nm}$ . To increase the pH value from 8.6 to 9.1, NaOH was added to the mother liquor and the mixture was stirred until the NaOH was dissolved. This was reflected in the specific surface area value. The BET area was smaller,  $515 \text{ m}^2/\text{g}$ , than expected for ZIF-8. These results may be due to the pH value of 8.6, which was lower than the initial value of 9.1.

### 3.4 Removal from CHLX—Batch Study

The design matrix of the uncoded values for the factors and the response in terms of the quantity of CHLX adsorbed per unit mass of ZIF-8 1G and ZIF-8 2G for all tests are presented in Table 3.

**Table 3** Results of the  $2^3$  factorial experimental for CHLX removal using ZIF-8 1G and ZIF-8 2G Experimental conditions: batch system,  $T = 25^\circ\text{C}$ ,  $\text{pH} = 6$ , agitation speed = 200 rpm.

Test	Agitation time (h)	Nanoadsorbent mass (g)	$C_0$ (mmol/L)	C (mmol/L)	ZIF-8 1G $q_e$ (mg/g)	ZIF-8 2G $q_e$ (mg/g)
1	1	0.04	0.05	0.020	18.95	18.32
2	6	0.04	0.05	0.019	20.85	18.95
3	1	0.06	0.05	0.021	13.48	11.79
4	6	0.06	0.05	0.017	14.32	13.48
5	1	0.04	0.07	0.034	30.96	26.54
6	6	0.04	0.07	0.033	28.43	27.17
7	1	0.06	0.07	0.036	19.37	16.85
8	6	0.06	0.07	0.032	21.06	18.53
9	3.5	0.05	0.06	0.024	19.71	18.20
10	3.5	0.05	0.06	0.024	20.22	18.20
11	3.5	0.05	0.06	0.024	20.22	17.69

It was also detected that for the adsorption capacity CHLX at equilibrium, i.e.,  $q_{eq}$  (amount of CHLX removed per gram of ZIF-8 1G), the best result was collected in test 5 carried out with higher agitation time, the best result being that of test 2, where 30.96 mg of CHLX are removed for every gram of ZIF-8 1G.

It was also detected that for the adsorption capacity CHLX at equilibrium, i.e.,  $q_{eq}$  (amount of CHLX removed per gram of ZIF-8 2G), the best result was collected in test 6 carried out with higher agitation time, the best result being that of test 2, where 27.17 mg of CHLX are removed for every gram of ZIF-8 2G.

One of the explanations for the adsorption capacity is the relationship between the pH and the zeta potential of the adsorbent. The point of zero charges ( $pH_{zpc}$ ) for ZIF-8 is approximately at pH 9.8, data reported in the literature [40]. The value of  $pH_{zpc}$  implied that the surface charge of the ZIF-8 nanoparticle was positive when the solution pH was below 9.8 and in this study the pH of the solution is 6.

The regression models (see Eq. (3)) demonstrate that the system is strongly dependent on Initial Concentration ( $C_0$ ) and nano-adsorbent mass ( $m$ ). The coefficient ( $R^2$ ) is equal to 99.92% for  $q_{eq}$ .

The adsorption capacity model of CHLX and regression equation for ZIF-8 1G (see Eq. (3)):

$$q_e = -25.31 + 6.78 * t + 452.8 * m + 1360.5 * C_0 - 115.8 * t * m - 149.5 * t * C_0 - 17901 * m * C_0 + 2633 * t * m * C_0 - 0.879 * P_t C_t \quad (3)$$

Where:  $q_{eq}$  is adsorption capacity (mg/g),  $t$  is the agitation time (h),  $m$  is the nano-adsorbent mass (g),  $C_0$  is the initial concentration (mmol/L),  $P_t C_t$  is the central point.

It should be noted that the coefficient had a value of  $R^2 = 99.94\%$ , showing that the model set out in Equation (3) fits the data well.

Figure 6 represents a standardized Pareto chart for effects (initial concentration, agitation time and nano-adsorbent mass) on the response (adsorption capacity).

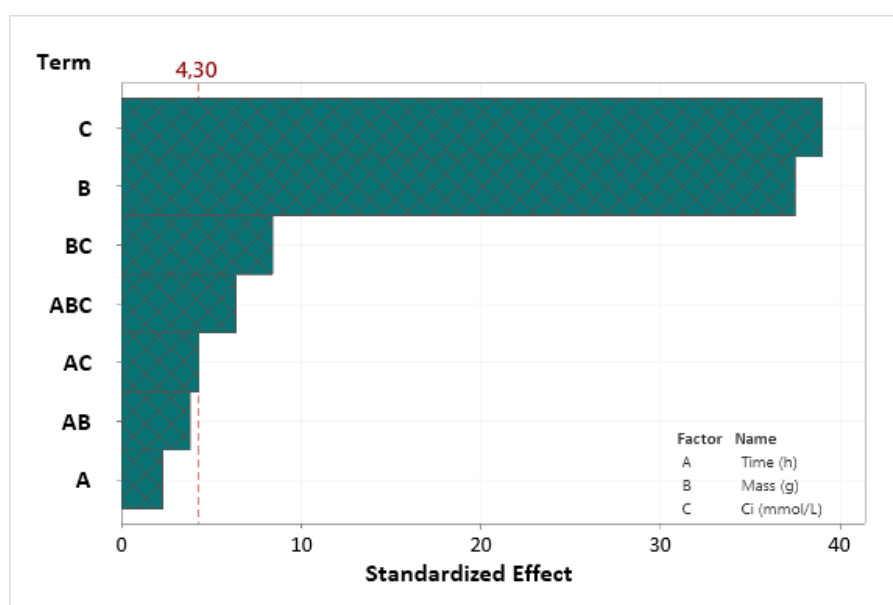


**Figure 6** Pareto chart for standardized effects for the initial concentration, agitation time and nano-adsorbent mass for ZIF-8 1G. Adsorption capacity,  $q_{eq}$ .

The initial concentration and nano-adsorbent mass plays a dominant effect on the adsorption capacity.

Figure 6 shows the Pareto chart for the standardized effects for CHLX adsorption at the 95% probability level. It is observed that the Initial Concentration ( $C_0$ ), agitation time ( $t$ ) and nano-adsorbent mass ( $m$ ) factors intersect the line of standardized effects.

The regression models (see Eq. (4)) demonstrate that the system is strongly dependent on Initial Concentration ( $C_0$ ) and nano-adsorbent mass ( $m$ ). The coefficient ( $R^2$ ) is equal to 99.92% for  $q_{eq}$ .

The adsorption capacity model of CHLX and regression equation for ZIF-8 2G (see Eq. (4)):

$$q_e = -4.66 - 0.31 * t + 58 * m + 726.8 * C_0 + 10.9 * t * m + 0.2 * t * C_0 - 7895 * m * C_0 - 5 * t * m * C_0 - 0.924 * P_t C_t \quad (4)$$

Where:  $q_{eq}$  is adsorption capacity (mg/g),  $t$  is the agitation time (h),  $m$  is the nano-adsorbent mass (g),  $C_0$  is the initial concentration (mmol/L),  $P_t C_t$  is the central point.

It should be noted that the coefficient had a value of  $R^2 = 99.92\%$ , showing that the model set out in Equation (5) fits the data well.

Figure 7 represents a standardized Pareto chart for effects (initial concentration, agitation time and nano-adsorbent mass) on the response (adsorption capacity).

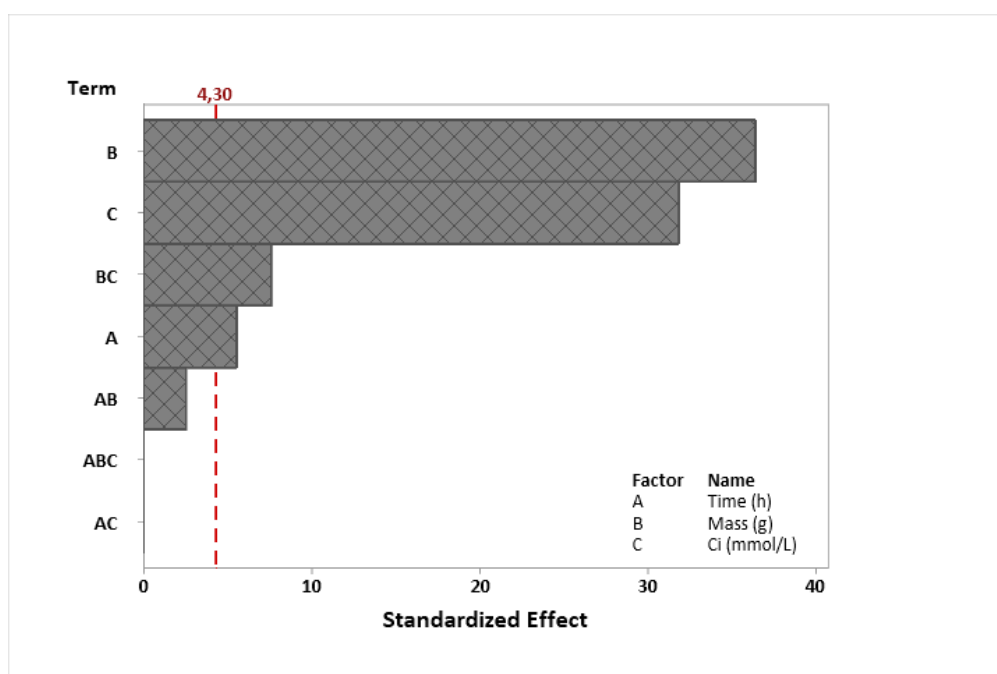


**Figure 7** Pareto chart for standardized effects for the initial concentration, agitation time and nano-adsorbent mass for ZIF-8 2G. Adsorption capacity,  $q_{eq}$ .

The initial concentration and nano-adsorbent mass play a dominant effect on the adsorption capacity.

Figure 7 shows the Pareto chart for the standardized effects for CHLX adsorption at the 95% probability level. It is observed that the Initial Concentration ( $C_0$ ), agitation time ( $t$ ) and nano-adsorbent mass ( $m$ ) factors intersect the line of standardized effects.

#### 4. Conclusions

ZIF-8 can be synthesized more economically and eco-friendly by reusing unreacted reagents (recycled synthesis solutions). Nanocrystals were prepared from two subsequent syntheses. The syntheses process using the mother liquor produced the structures of the ZIF-8 in the two generations, as determined by X-ray diffractograms (XRD), which showed high purity.

The effects of process factors such as initial concentration ( $C_0$ ), agitation time ( $t$ ) and nano-adsorbent mass ( $m$ ) were studied.

The model's predictions developed based on the 2<sup>3</sup> factorial experimental were excellent in the experimental range evaluated. The results indicated that the initial concentration of CHLX and nano-adsorbent mass influenced the adsorption capacity.

### **Acknowledgments**

The authors gratefully acknowledge to the CNPq (Conselho Nacional de Pesquisa e Desenvolvimento) and Coordenação de Aperfeiçoamento de Pessoal de Nível Superior (CAPES) for the financial support. We thank Laboratory of Multifunctional Materials and Nanocomposites LAMMEN-ECT UFRN for the FTIR analysis.

### **Author Contributions**

Heloísa M. Oliveira: Investigation, Formal analysis, Writing – Original Draft; Francisco A. S. Silva: Investigation: Investigation, Formal analysis; Tellys L. A. Barbosa: Investigation, Formal analysis; Meiry G. F. Rodrigues: Conceptualization, Formal analysis, Funding acquisition, Writing – Review & Editing.

### **Funding**

Conselho Nacional de Desenvolvimento Científico e Tecnológico (CNPq) and Coordenação de Aperfeiçoamento de Pessoal de Nível Superior (CAPES).

### **Competing Interests**

The authors have declared that no competing interests exist.

### **References**

1. Wilkinson JL, Boxall AB, Kolpin DW, Leung KM, Lai RW, Galbán-Malagón C, et al. Pharmaceutical pollution of the world's rivers. *Proc Natl Acad Sci.* 2022; 119: e2113947119.
2. Lv SW, Liu JM, Wang ZH, Ma H, Li CY, Zhao N, et al. Recent advances on porous organic frameworks for the adsorptive removal of hazardous materials. *J Environ Sci.* 2019; 80: 169-185.
3. Meng Y, Liu W, Liu X, Zhang J, Peng M, Zhang T. A review on analytical methods for pharmaceutical and personal care products and their transformation products. *J Environ Sci.* 2021; 101: 260-281.
4. Afonso-Olivares C, Sosa-Ferrera Z, Santana-Rodríguez JJ. Occurrence and environmental impact of pharmaceutical residues from conventional and natural wastewater treatment plants in Gran Canaria (Spain). *Sci Total Environ.* 2017; 599: 934-943.
5. Le-Minh N, Khan SJ, Drewes JE, Stuetz RM. Fate of antibiotics during municipal water recycling treatment processes. *Water Res.* 2010; 44: 4295-4323.
6. Brun GL, Bernier M, Losier R, Doe K, Jackman P, Lee HB. Pharmaceutically active compounds in Atlantic Canadian sewage treatment plant effluents and receiving waters, and potential for environmental effects as measured by acute and chronic Aquatic Toxicity. *Environ Toxicol Chem.* 2006; 25: 2163-2176.

7. Kolpin DW, Furlong ET, Meyer MT, Thurman EM, Zaugg SD, Barber LB, et al. Pharmaceuticals, hormones, and other organic wastewater contaminants in U.S. streams, 1999-2000: A national reconnaissance. *Environ Sci Technol.* 2002; 36: 1202-1211.
8. Patel M, Kumar R, Kishor K, Mlsna T, Pittman Jr CU, Mohan D. Pharmaceuticals of emerging concern in aquatic systems: Chemistry, occurrence, effects, and removal methods. *Chem Rev.* 2019; 119: 3510-3673.
9. Seo PW, Bhadra BN, Ahmed I, Khan NA, Jung SH. Adsorptive removal of pharmaceuticals and personal care products from water with functionalized metal-organic frameworks: Remarkable adsorbents with hydrogen-bonding abilities. *Sci Rep.* 2016; 6: 34462.
10. Ighalo JO, Rangabhashiyam S, Adeyanju CA, Ogunniyi S, Adeniyi AG, Igwegbe CA. Zeolitic imidazolate frameworks (ZIFs) for aqueous phase adsorption – A review. *J Ind Eng Chem.* 2022; 105: 34-48.
11. Venna SR, Jasinski JB, Carreon MA. Structural evolution of zeolitic imidazolate framework-8. *J Am Chem Soc.* 2010; 132: 18030-18033.
12. Wagner M, Lin KY, Oh WD, Lisak G. Metal-organic frameworks for pesticidal persistent organic pollutants detection and adsorption – A mini review. *J Hazard Mater.* 2021; 413: 125325.
13. Chen LJ, Luo B, Li WS, Yang C, Ye T, Li SS, et al. Growth and characterization of zeolitic imidazolate framework-8 nanocrystalline layers on microstructured surfaces for liquid crystal alignment. *RSC Adv.* 2016; 6: 7488-7494.
14. Park KS, Ni Z, Côté AP, Choi JY, Huang R, Uribe-Romo FJ, et al. Exceptional chemical and thermal stability of zeolitic imidazolate frameworks. *Proc Natl Acad Sci.* 2006; 103: 10186-10191.
15. Schejn A, Balan L, Falk V, Aranda L, Medjahdi G, Schneider R. Controlling ZIF-8 nano- and microcrystal formation and reactivity through zinc salt variations. *Cryst Eng Comm.* 2014; 16: 4493-4500.
16. Yuan J, Li Q, Shen J, Huang K, Liu G, Zhao J, et al. Hydrophobic-functionalized ZIF-8 nanoparticles incorporated PDMS membranes for high-selective separation of propane/nitrogen. *Asia-Pac J Chem Eng.* 2017; 12: 110-120.
17. Cravillon J, Münzer S, Lohmeier SJ, Feldhoff A, Huber K, Wiebcke M. Rapid room-temperature synthesis and characterization of nanocrystals of a prototypical zeolitic imidazole framework. *Chem Mater.* 2009; 21: 1410-1412.
18. Shahsavari M, Jahani PM, Sheikhshoaei I, Tajik S, Afshar AA, Askari MB, et al. Green synthesis of zeolitic imidazolate frameworks: A review of their characterization and industrial and medical applications. *Materials.* 2022; 15: 447.
19. Gökpınar S, Diment T, Janiak C. Environmentally benign dry-gel conversions of Zr-based UiO metal-organic frameworks with high yield and the possibility of solvent re-use. *Dalton Trans.* 2017; 46: 9895-9900.
20. Palacín MG, Martínez JI, Paseta L, Deacon A, Johnson T, Malankowska M, et al. Sized-controlled ZIF-8 nanoparticle synthesis from recycled mother liquors: Environmental impact assessment. *ACS Sustain Chem Eng.* 2020; 8: 2973-2980.
21. Li H, Chen W, Liu B, Yang M, Huang Z, Sun C, et al. A purely green approach to low-cost mass production of zeolitic imidazolate frameworks. *Green Energy Environ.* 2021. doi: 10.1016/j.gee.2021.09.003.
22. Şahin F, Topuz B, Kalipçılar H. Synthesis of ZIF-7, ZIF-8, ZIF-67 and ZIF-L from recycled mother liquors. *Microporous Mesoporous Mater.* 2018; 261: 259-267.



23. Barbosa TSB, Barros TRB, Barbosa TLA, Rodrigues MGF. Green synthesis for MCM-41 and SBA-15 silica using the waste mother liquid. *Silicon*. 2022; 14: 6233-6243.
24. Ahmad K, Nazir MA, Qureshi AK, Hussain E, Najam T, Javed MS, et al. Engineering of Zirconium based metal-organic frameworks (Zr-MOFs) as efficient adsorbents. *Mater Sci Eng*. 2020; 262: 114766.
25. Ahmad K, Shah H-u-R, Ashfaq M, Shah SSA, Hussain E, Naseem HA, et al. Effect of metal atom in zeolitic imidazolate frameworks (ZIF-8 & 67) for removal of  $Pb^{2+}$  &  $Hg^{2+}$  from water. *Food Chem Toxicol*. 2021; 149: 112008.
26. Ahmad K, Shah HR, Ahmad M, Ahmed MM, Naseem K, Riaz NN, et al. Comparative study between two zeolitic imidazolate frameworks as adsorbents for removal of organoarsenic, As(III) and As(V) species from water. *Braz J Anal Chem*. 2022; 9: 78-97.
27. Dai H, Yuan X, Jiang L, Wang H, Zhang J, Zhang J, et al. Recent advances on ZIF-8 composites for adsorption and photocatalytic wastewater pollutant removal: Fabrication, applications and perspective. *Coord Chem Rev*. 2021; 441: 213985.
28. Ferraz LRM, Tabosa AEGA, Nascimento DDSS, Ferreira AS, Sales VAW, Silva JYR, et al. ZIF-8 as a promising drug delivery system for benzimidazole: development, characterization, in vitro dialysis release and cytotoxicity. *Sci Rep*. 2020; 10:16815. doi: 10.1038/s41598-020-73848-w
29. Wang Q, Sun Y, Li S, Zhang P, Yao Q. Synthesis and modification of ZIF-8 and its application in drug delivery and tumor therapy. *RSC Adv*. 2020; 10: 37600-37620. doi: 10.1039/d0ra07950b.
30. Fent K, Weston AA, Caminada D. Ecotoxicology of human pharmaceuticals. *Aquat Toxicol*. 2006; 76: 122-159.
31. Supranoto SC, Slot DE, Addy M, Van der Weijden GA. The effect of chlorhexidine dentifrice or gel versus chlorhexidine mouthwash on plaque, gingivitis, bleeding and tooth discoloration: A systematic review. *Int J Dent Hyg*. 2015; 13: 83-92.
32. Montgomery DC, Runger GC. Applied statistics and probability for engineers. New York: John Wiley & Sons; 2003.
33. Rodrigues MGF, Barbosa TLA, Rodrigues DPA. Zinc imidazolate framework-8 nanoparticle application in oil removal from oil/water emulsion and reuse. *J Nanopart Res*. 2020; 22: 328.
34. Sann EE, Pan Y, Gao Z, Zhan S, Xia F. Highly hydrophobic ZIF-8 particles and application for oil-water separation. *Sep Purif Technol*. 2018; 206: 186-191.
35. Cho HY, Kim J, Kim SN, Ahn WS. High yield 1-L scale synthesis of ZIF-8 via a sonochemical route. *Microporous Mesoporous Mater*. 2013; 169: 180-184.
36. Zhang H, James J, Zhao M, Yao Y, Zhang Y, Zhang B, et al. Improving hydrostability of ZIF-8 membranes via surface ligand exchange. *J Membr Sci*. 2017; 532: 1-8.
37. Zhang H, Liu D, Yao Y, Zhang B, Lin YS. Stability of ZIF-8 membranes and crystalline powders in water at room temperature. *J Membr Sci*. 2015; 485: 103-111.
38. Zhang H, Zhao M, Lin YS. Stability of ZIF-8 in water under ambient conditions. *Microporous Mesoporous Mater*. 2019; 279: 201-210.
39. Bhattacharjee S, Jang MS, Kwon HJ, Ahn WS. Zeolitic imidazolate frameworks: Synthesis, functionalization, and catalytic/adsorption applications. *Catal Surv From Asia*. 2014; 18: 101-127.
40. Li J, Wu YN, Li ZH, Zhang BR, Zhu M, Hu X, et al. Zeolitic imidazolate framework-8 with high efficiency in trace arsenate adsorption and removal from water. *J Phys Chem C*. 2014; 118: 27382-27387.